Pictorial Essay

Large airway diseases in pediatrics: a pictorial essay

Acta Radiologica Open
9(12) 1–11

DOI: 10.1177/2058460120972694
journals.sagepub.com/home/arr
SAGE

Spyridon Prountzos[1], Olympia Papakonstantinou[1], Vasiliki Bizimi[1], Georgios Velonakis[1], Argyro Mazioti[1], Konstantinos Douros[2] and Efthymia Alexopoulou[1]

Abstract

"Large airway diseases" is being used as an all-encompassing phrase to describe a broad spectrum of pathological entities, which involves the trachea, main, lobar, and segmental bronchi of up to 3 mm diameter. Imaging modalities such as radiography, computed tomography, and magnetic resonance imaging contribute to the identification and diagnosis of each entity. Knowledge of clinical information, normal cross-sectional anatomy, and imaging characteristics of large airway diseases is necessary for appropriate radiologic evaluation. This review provides information about congenital and acquired diseases of the large airways in the pediatric population.

Keywords

Chest, airways, pediatric, CT, trachea, bronchi

Received 10 May 2020; accepted 21 October 2020

Introduction

Technological advances both in hardware and software for the past 20 years have allowed cutting-edge technology to be implemented in the daily routine of radiologists, to achieve reaching the diagnosis of pathological entities that would otherwise require the use of interventional techniques to be diagnosed with. Such an example is large airway diseases. "Large airway diseases" is an umbrella phrase used to describe a spectrum of pathology of the tracheobronchial tree up to the level of segmental bronchi. Imaging in pediatrics requires fast acquisition times, high spatial resolution for anatomical coverage, and reduced need for sedation. Computed tomography (CT) and magnetic resonance imaging (MRI) have revolutionized the noninvasive imaging of large airways by combining the abovementioned requirements. Multi-detector computed tomography (MDCT) enabled the production of high-resolution two- (2D) and three-dimensional (3D) multiplanar reconstructions (MPRs) for evaluation of even the smallest of lesions. Ciné-CT and newer techniques such as four-dimensional (4D) CT can be implemented to evaluate dynamic phenomena. 4D-CT scanning is leveraging motion during the respiratory cycle and combines it into a multiphase, dynamic dataset to answer important clinical questions such as tracheobronchomalacia, and study complex vascular rings and slings. However, high radiation doses may deem unsuitable the use of this technique, whereas MRI can provide the same information without the use of ionizing radiation. Advances in the development of Ultrashort Echo Time sequences are creating high expectations because of their inherent ability to address the three main barriers concerning the thoracic imaging in MRI, namely respiratory- and cardiac-related motion, low proton density, and fast signal decay due to innumerable susceptibility artifacts at air–tissue interfaces.

[1]2nd Department of Radiology, National and Kapodistrian University of Athens, "Attikon" University Hospital of Athens, Athens, Greece
[2]Allergology and Pulmonology Unit, 3rd Pediatric Department, Attikon Hospital, National and Kapodistrian University of Athens, Athens, Greece

Corresponding author:
Spyridon Prountzos, 2nd Department of Radiology, National and Kapodistrian University of Athens, "Attikon" University Hospital of Athens, Athens, Greece.
Email: spyttt@gmail.com

Tracheobronchial tree

Anatomy: embryology

The trachea is a semiflexible tube extending from the lower portion of the larynx at the level of sixth to seventh cervical vertebra to the carina approximately at the level of fourth to fifth thoracic vertebra, where it bifurcates to form the main bronchi for the lungs. In pediatric patients, the larynx is anterior and cephalad (C3-4 vs C6) and the trachea and neck are short. Its total length can reach up to about 10–13cm and diameter up to 2 cm. Histologically, it consists of 16–2 incomplete crescentic-shaped cartilaginous rings, which form its anterior and lateral walls, and smooth muscle and adventitial layer at the posterior side. During the fourth week of embryonic development, the trachea starts to shape from the ventral foregut epithelium forming the tracheobronchial diverticulum, which will later continue budding caudally to form the tracheobronchial tree.[1]

Large airway diseases

Differential diagnoses for large airway diseases are listed in Table 1. Bronchiectasis is not going to be discussed in this pictorial essay.

Congenital anomalies

Congenital large airway diseases can be divided in two main categories: (1) Static anomalies, which remain unchanged during the examination and (2) dynamic anomalies, which are distinguished by continuous change and require special examination protocols to better visualize them.

Static anomalies

Intrinsic lesions

Tracheobronchial branching anomalies. Tracheobronchial branching malformations or variants are as frequent as 12% in adults undergoing bronchoscopy, with the numbers further increasing when using modern imaging modalities. The two most common congenital anomalies are ectopic and supernumerary bronchi. Ectopic bronchi are more common than supernumerary ones. The most prevalent type of ectopic bronchus is the tracheal bronchus, a term used to describe bronchi originating from the outer tracheal or main bronchial wall and, directed to, the upper lobe (Fig. 1). Tracheal bronchus can be characterized as either displaced if the anatomic upper-lobe bronchus is missing a single branch or supernumerary if the upper-lobe bronchus has a normal trifurcation. There is an association with tracheal stenosis distally to the tracheal bronchus location. The accessory cardiac bronchus is a frequent supernumerary bronchus arising from the inner wall of the right main or intermediate bronchus opposite to the

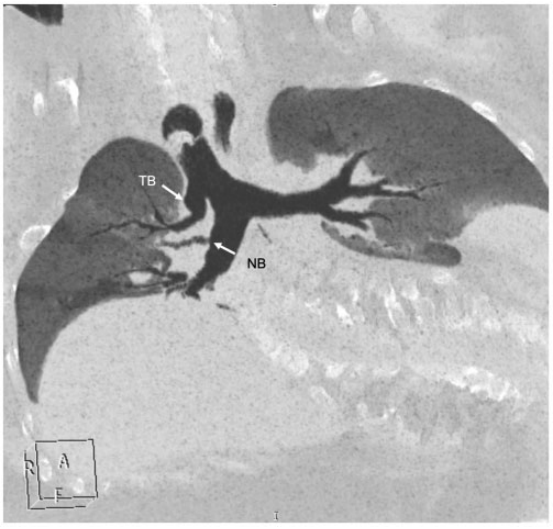

Fig. 1. Coronal MPR showing a 17-year-old boy with right displaced tracheal bronchus (TB) for the posterior and apical segments and a normal bronchus (NB) for the RUL supplying the anterior segment, arising from the right main bronchus. The patient also exhibits noted scoliosis due to his underlying condition of arthrogryposis. $CTDI_{vol} = 4.5$ mGy.

Table 1. Large airway diseases.

Congenital				Acquired
Static			Dynamic	
Intrinsic	Extrinsic		Tracheobronchomalacia	Tracheobronchomalacia Tracheobronchial fistula
Tracheobronchial branching anomalies	**Non-Vascular**	**Vascular**		Tracheal stenosis
Pulmonary agenesis, aplasia, or hypoplasia	Foregut duplication cysts	Vascular rings		Foreign body aspiration
Bronchial atresia	Tracheobronchial fistula	Pulmonary artery slings		Neoplasms
Tracheal stenosis				Inflammatory

origin of the right upper lobe. CT scan is the modality of choice, although chest radiography may sometimes reveal such pathology.[1,2,4]

Pulmonary agenesis, aplasia, or hypoplasia. Congenital bronchial underdevelopment in the form of either pulmonary agenesis, aplasia, or hypoplasia is of yet unknown fetal pathophysiology. Pulmonary agenesis is accompanied by a complete lack of bronchial structures, lung parenchyma, as well as, vascular supply. Agenesis can be associated with tracheal stenosis due to formation of complete tracheal rings. Pulmonary aplasia consists of a rudimentary bronchus, along with incomplete lung development (Fig. 2). In pulmonary hypoplasia, the bronchus is also rudimentary with a hypoplastic lung. Vascular supply in these two latter forms is either hypoplastic or absent. Initial investigation is by chest radiography, followed by CT scan.[2,3]

Bronchial atresia. This refers to the congenital obliteration of a bronchial segment followed by normal development of its proximal and distal airway. More frequently, it appears to the left upper lobe. The airway distal to the obliterated segment is dilated and filled with mucus, forming a V- or Y-shaped tubular opacity, surrounded by hypoattenuated lung parenchyma due to air-trapping, especially appreciated using minimum intensity projection on a CT scan (Fig. 3). Bronchial atresia can be associated with other prenatal lung malformations including congenital pulmonary airway malformation, pulmonary sequestration. Initial investigation is by chest radiography, while CT may follow for a detailed study.[5,6,9]

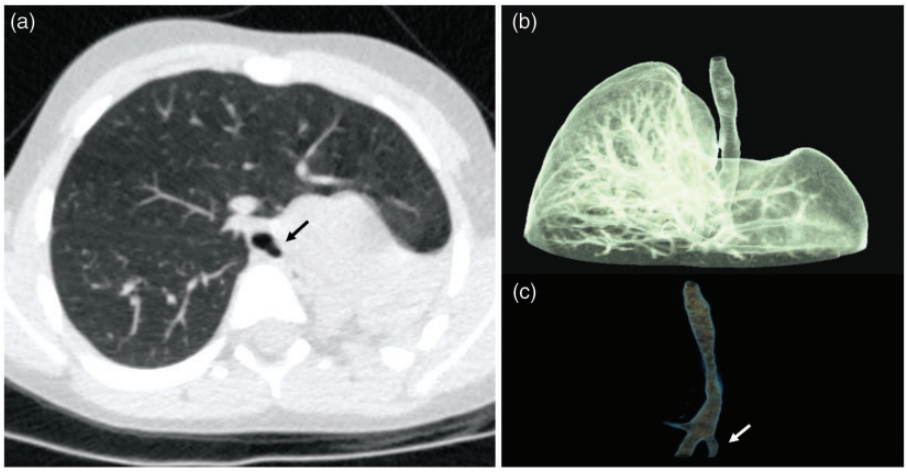

Fig. 2. (a) Axial CT image of a 5-year-old boy with left lung aplasia showing the hyperinflated right pulmonary parenchyma and the rudimentary left main bronchus (black arrow). (b and c) 3D volume-rendering technique (VRT) shows the rudimentary left main bronchus (white arrow). $CTDI_{vol} = 1.1$ mGy.

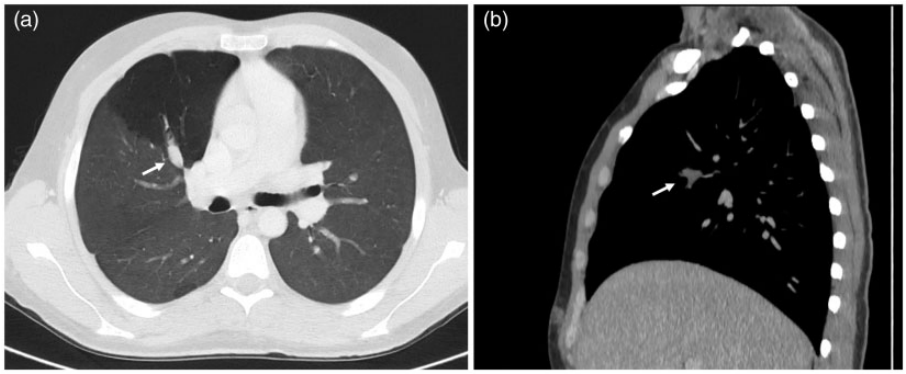

Fig. 3. Bronchial atresia as an incidental finding in a 16-year-old male. (a) Axial minimum intensity projection CT image depicting the atretic right anterior segmental bronchus dilated and filled with mucus (arrow), surrounded by hypo-attenuated lung parenchyma due to air-trapping. (b) Sagittal CT image showing the characteristic Y-shaped atretic anterior segmental bronchus filled with mucous (arrow). $CTDI_{vol} = 4.3$ mGy (combined chest–abdomen–pelvis examination).

Tracheal stenosis. Congenital tracheal stenosis refers to existence of complete or near-complete cartilaginous rings without tracheal wall thickening. Typical radiological findings include a diffuse or focal, funnel-like progressive reduction of the tracheal luminal diameter (Fig. 4). Severe forms of stenosis occupying a greater length are usually symptomatic from the early neonatal age, largely associated with vascular rings and pulmonary artery slings. Acquired tracheal stenosis caused by prolonged endotracheal or tracheostomy tubing or surgery is seen as a focal narrowing of the proximal tracheal lumen with eccentric or concentric soft tissue thickening due to pressure necrosis, ischemia, and fibrosis. High-kV chest radiography may reveal the suspected pathology. CT scan is considered the gold standard modality.[2,3,5-7,9,10]

Extrinsic lesions

Non-vascular lesions

Foregut duplication cysts. They arise during pulmonary development due to abnormal budding of the embryonic foregut and the tracheobronchial tree. They are characterized by an isolated portion of lung tissue communicating with the upper gastrointestinal tract or the central nervous system in the form of a bronchogenic, enteric, or neurenteric cyst, respectively. Radiologic appearance varies but generally, they resemble thin-walled cystic lesions with homogeneous content showing no contrast enhancement, unless there is an underlying active inflammatory process (Fig. 5). CT is considered the modality of choice. MRI is an alternative technique to depict the pathology especially if clarification of the cystic contents' nature is needed when CT reveals attenuation higher than water or contrast enhancement cannot be objectively excluded. Dual-energy CT may be helpful in this regard using material decomposition techniques.[2,7,13,15]

Tracheoesophageal fistula. Tracheoesophageal fistula consists of an abnormal communication between the tracheal and the esophageal lumen. Such fistulas coexist with esophageal atresia and they are diagnosed postnatally. The congenital form shows higher incidence in congenital cardiac, urogenital, and gastrointestinal malformations (Fig. 6). The acquired form is associated with previous infections, trauma, or swallowing of corrosive materials such as batteries (Fig. 7) and neoplasms. Esophagogram is the gold-standard technique, but MDCT scan may be additionally needed.[3,5,7,16]

Vascular lesions

Vascular rings and slings. Congenital vascular malformations of the great vessels of the mediastinum constitute a common cause of respiratory distress. A vascular *ring* is defined as a developmental abnormality of the aortic arch, its branches or remnants that surround the esophagus and the trachea resulting in compression. A pulmonary artery sling is defined as an abnormal origin of the left pulmonary artery from the right pulmonary artery with its course between the trachea and the esophagus. The most common malformations are listed in Table 2. The anomalous vascular structure can either surround or leave an indentation to the trachea, the esophagus, or both leading to external compression and respiratory and/or dysphagia (Fig. 8). The investigation may include an esophagogram in cases presenting with dysphagia, which may be indicative of the presence of vascular rings/slings, although this technique tends to be abandoned. CT or MR angiography can be the first investigative study.[2–4,7,11,12,14]

Dynamic large airway abnormality

Tracheobronchomalacia

Tracheobronchomalacia refers to the excessive flattening of the tracheal lumen or the main bronchi, due to

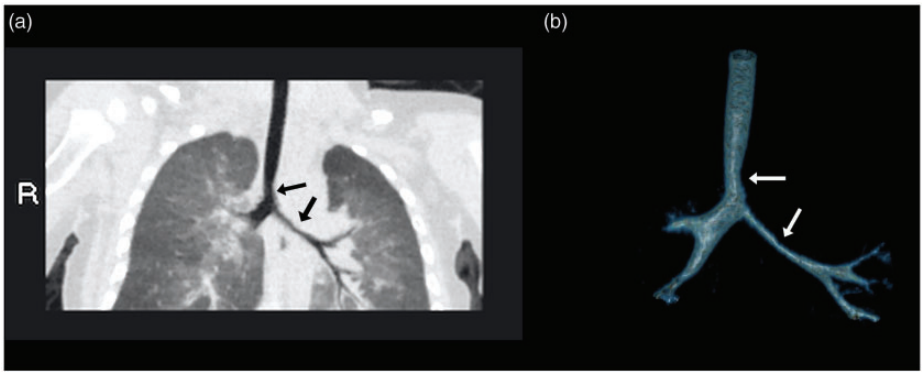

Fig. 4. (a) Coronal minimum intensity projection and (b) 3D volume-rendering technique on a 7-month-old boy with mild congenital stenosis of the distal trachea and more prominent of the left main bronchus (arrows). Mosaic appearance of lung parenchyma due to air trapping can be appreciated. Tracheal stenosis was confirmed by flexible bronchoscopy. $CTDI_{vol} = 1.88$ mGy.

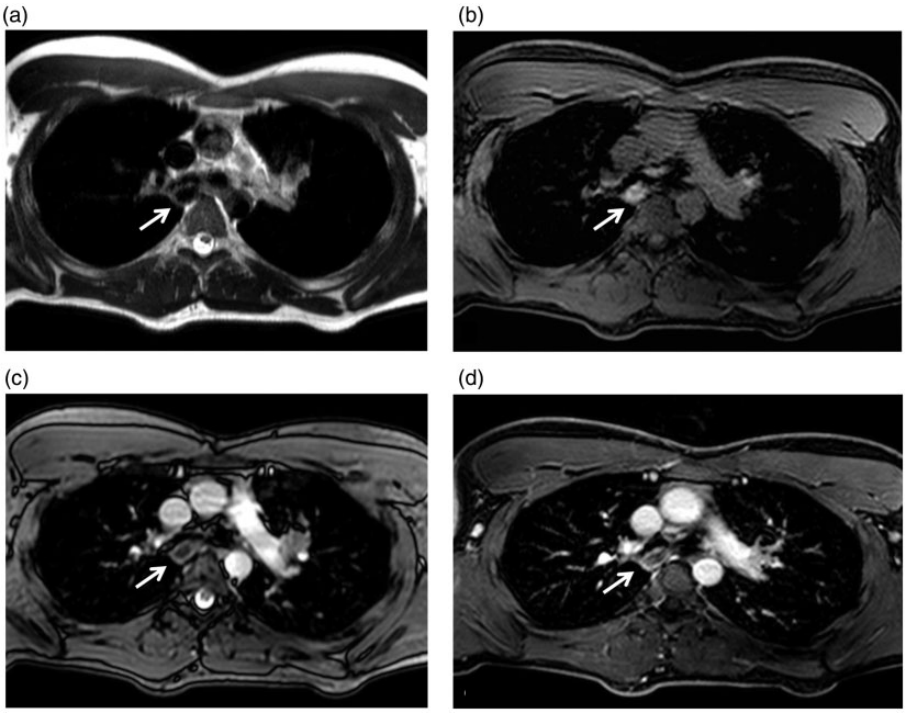

Fig. 5. Bronchogenic cyst in a 10-year-old boy. MRI scan shows a thin-walled cystic lesion (arrow) with protein content in contact with the anteriorly displaced right main bronchus on (a) axial T2WI, (b) axial T1WI FatSat, and (c) axial BTFE studies, which do not show contrast enhancement on (d) T1WI FatSat post-gadolinium injection.

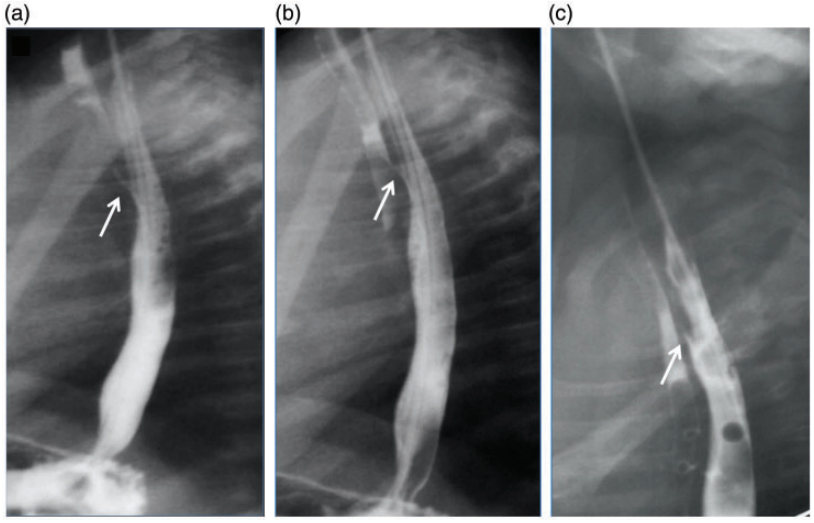

Fig. 6. Esophagogram of a 20-day-old male revealing a congenital tracheoesophageal fistula (arrow). DLP = not available.

"weakening" of the cartilaginous rings and/or, the posterior muscular wall. The congenital form is highly associated with gestational prematurity, the concurrent existence of a tracheoesophageal fistula, or underlying chondropathies. The acquired form is related to previous infection, intubation or surgery and, extrinsic compression, mediastinal vascular malformations. A paired end-inspiration/forced-expiration protocol is required to demonstrate the pathology when performing a CT scan. When available, ciné-CT or a more recent 4D-CT protocol should be implemented to accurately assess the tracheal lumen wall dynamics. Gapless 4D-CT imaging can be performed either during free breathing or with additional respiratory maneuvers, such as cough, while assessing the complex movement of nearby structures and their effect on the tracheal

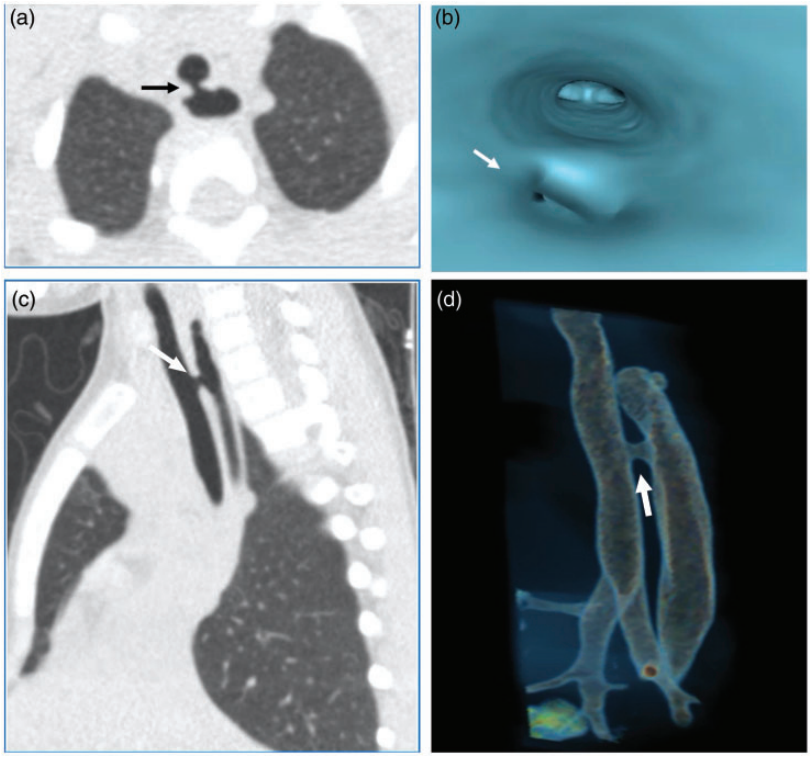

Fig. 7. Chest CT on an 8-year-old boy shows the communication (arrow) between the trachea and the esophagus, and the formation of an acquired tracheoesophageal fistula. $CTDI_{vol} = 2.2$ mGy.

Table 2. Vascular ring and pulmonary artery sling types.

Double aortic arch: right dominant, left dominant, and co-dominant
Right aortic arch with aberrant left subclavian artery
Right aortic arch with mirror image branching and retroesophageal ductus arteriosus
Circumflex aortic arch
Innominate artery compression
Pulmonary artery sling (types I and II)

wall, thus making the evaluation of the extent and severity of tracheomalacia more straightforward. The diagnostic criterion is at least 50% reduction of the anteroposterior diameter of the tracheal lumen on expiration (Fig. 9). Recent studies introduce the use of dynamic MRI as an alternative non-ionizing technique.[2,3,8,16–18]

Acquired diseases

Foreign body aspiration. The right bronchial tree, due to its morphology, is the most frequent location of foreign body aspiration. Radiolucent foreign bodies (90% of the cases, e.g. food) can prove quite elusive to demonstrate directly with chest radiography, thus searching for secondary characteristics as aspiration can be accompanied by atelectasis or air-trapping, on inspiratory/expiratory studies. CT scan is useful when searching both radiolucent and radiopaque foreign bodies and chest radiography studies are inconclusive (Fig. 10).[2,6,8,19–21]

Neoplasms. Large airway neoplasms are classified into two categories: (1) primary neoplasms, arising directly from the airways and (2) secondary, located outside the airways but in close proximity thus causing extrinsic compression or directly infiltrating them. Although initial diagnostic work-up begins with a chest radiography, further investigation with CT or MRI (with intravenous contrast injection) is mandatory.

Primary neoplasms are further categorized as benign and malignant. Benign neoplasms appear as focal, well-defined, intramural lesions without infiltration of the tracheal wall or other mediastinal structures. Hemangiomas and papillomas are the two most frequent lesions. Radiologically, a typical hemangioma consists a round, well-defined, contrast-enhancing, soft-tissue density lesion, usually located in the sublingual or upper tracheal region, normally in the neonatal age. Tracheobronchial papillomatosis is caused by the human papilloma virus and usually involves the larynx, but it can spread to the trachea and bronchi. It presents as multiple nodular lesions projecting into the tracheal lumen or as diffuse nodular wall thickening (Fig. 11).

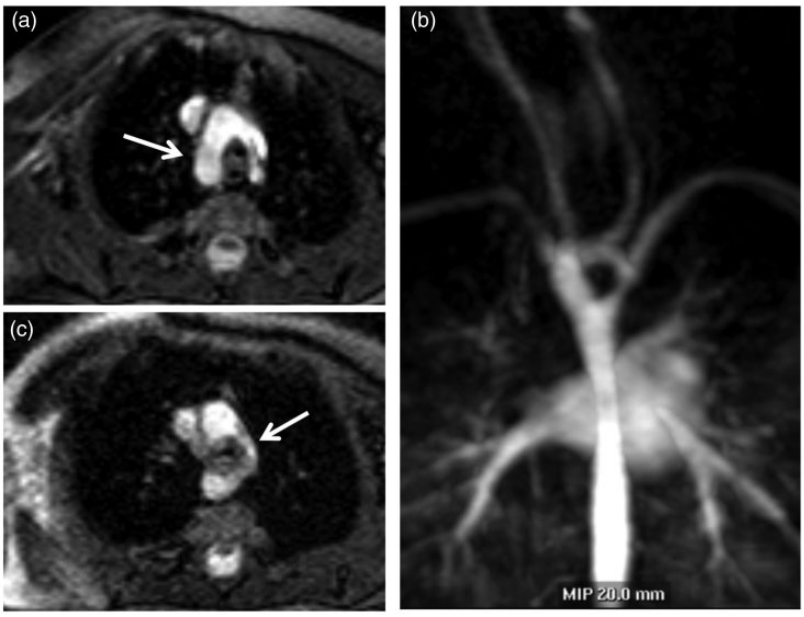

Fig. 8. Chest MR angiography showcasing a double aortic arch on a 4-month-old male surrounding and compressing the trachea. (a and b) Axial T1WI post-gadolinium injection MR angiography and (c) coronal maximum-intensity projection.

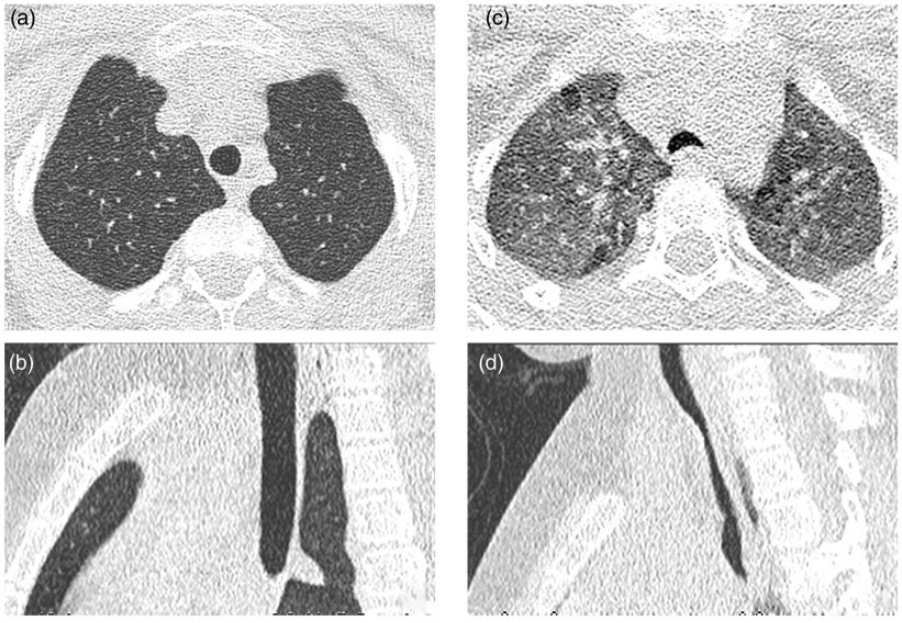

Fig. 9. Acquired tracheomalacia. Paired end-inspiratory/forced-expiratory CT. (a and b) End-inspiration phase and (c and d) forced-expiration phase show significant expiratory reduction in the cross-sectional luminal area of the trachea (arrow). Mosaic appearance of the apical lung parenchyma due to air trapping can be appreciated. $CTDI_{vol} = 2.47$ mGy (inspiration) and 2.41 mGy (expiration).

The two most common malignant pediatric tumors are the carcinoid tumor and the mucoepidermoid carcinoma. Carcinoid tumor is a neuroendocrine tumor excreting hormone, which typically arises within the main or lobar bronchi, making curved 2D MPRs suitable for its demonstration. Mucoepidermoid carcinoma typically occurs in the main or proximal lobar bronchus, measures up to 4 cm in diameter, and has a polypoid appearance.

Secondary neoplasms include primary lymphoma and metastatic mediastinal lymphadenopathy. Hematogenous spread from distant neoplasms directly to large airways is extremely rare in pediatric patients. Lymphoma consists of the Hodgkin and Non-Hodgkin

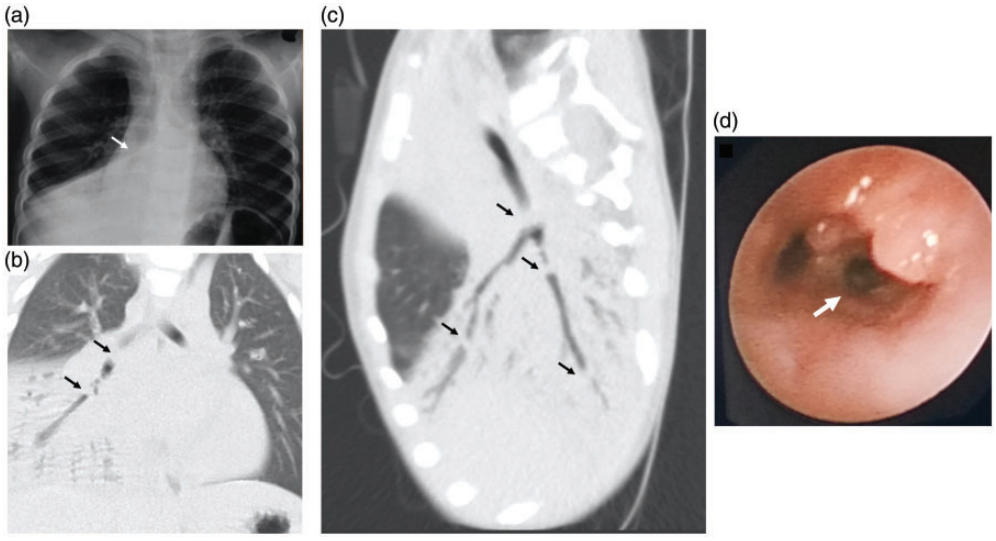

Fig. 10. Foreign body aspiration (crushed nuts) in a 3-year-old boy on (a) chest radiography. (b and c) CT images showing multiple opacities inside the tracheobronchial tree (arrows) with peripheral lung collapse. (d) Bronchoscopic image showing part of nut swallowed. $CTDI_{vol} = 0.83$ mGy.

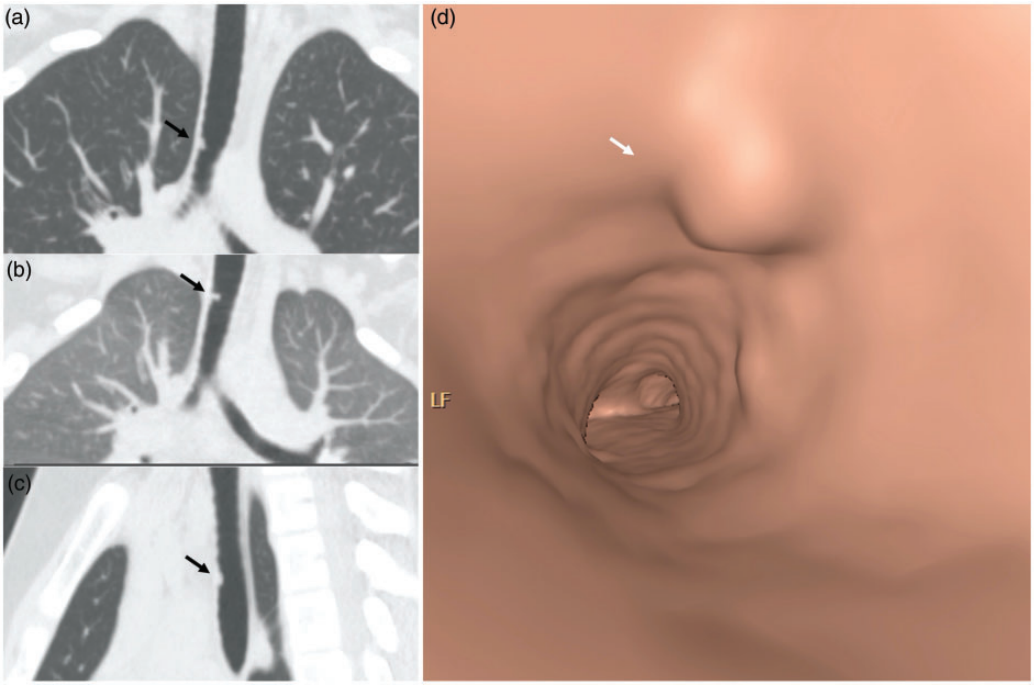

Fig. 11. Incidental finding of papillomatous lesions on the tracheal wall. (a and b) Coronal and (c) sagittal CT image showing multiple nodular lesions (black arrows) projecting into the tracheal lumen. (d) Virtual bronchoscopy showcasing one of the papillomatous lesion (white arrow). $CTDI_{vol} = 1.9$ mGy (inspiration) and 0.52 mGy (expiration).

type, with the former having a higher prevalence on the first decade of life and the latter having the same prevalence on the first and second decades of life. They often cause mass effect and extrinsic compression of the trachea. Metastatic mediastinal lymphadenopathy arises from neuroblastomas (Fig. 12), Wilms tumor, testicular neoplasms and sarcomas. They present as homogenous, nodular soft tissue conglomerates, showing contrast enhancement and occasionally hypoattenuating–necrotic center and/or calcifications. Highly aggressive tumors can cause extrinsic compression or airway invasion.[3,5,6,8,15,22,23]

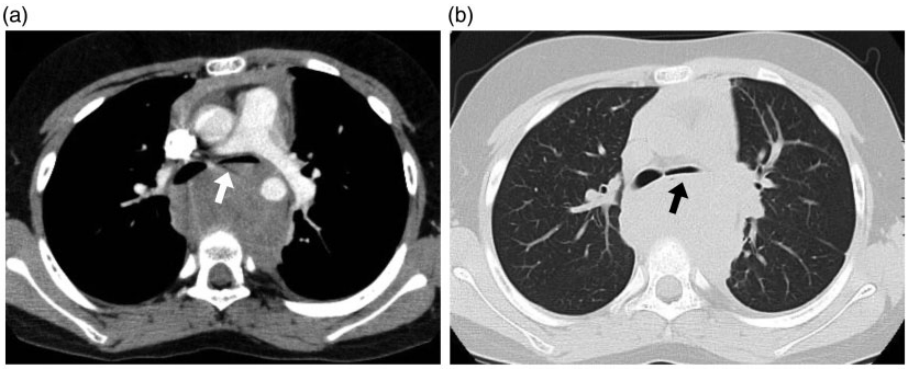

Fig. 12. Neuroblastoma on a 9-year-old boy. (a and b) Axial CT image shows noted anterior displacement of the posterior mediastinal compartment and compression of the left main bronchus (arrow) due to mass effect from soft tissue mass, which encases the descending aorta. $CTDI_{vol} = 3.6$ mGy (combined chest–abdomen–pelvis study).

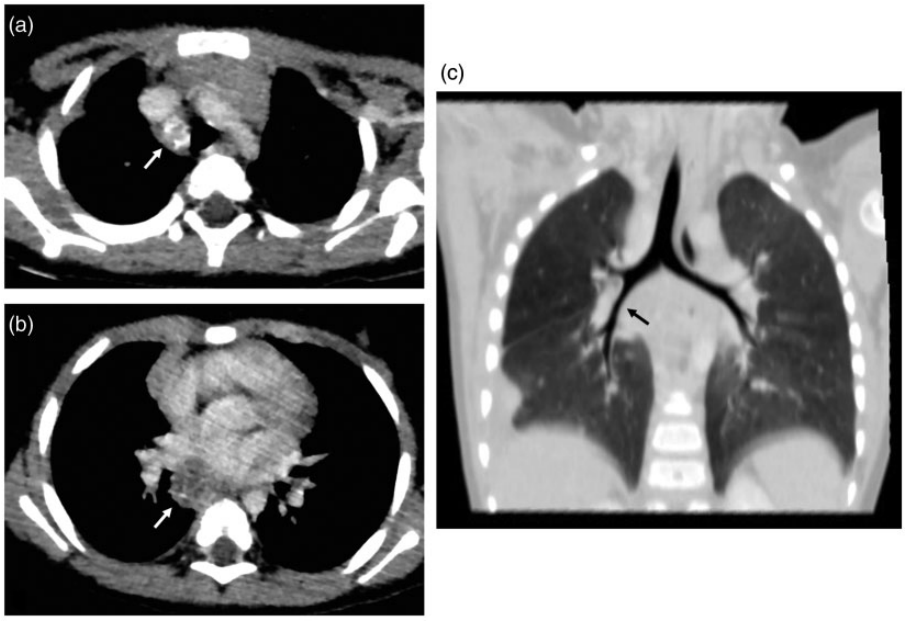

Fig. 13. Mediastinal lymphadenopathy in a 9-month-old girl due to tuberculosis infection. (a and b) Axial CT images post-IV-contrast injection show lymph node conglomerates with necrosis and calcifications (white arrows) and (c) mild compression of the right intermediate bronchus (black arrow). $CTDI_{vol} = 1.52$ mGy.

Inflammatory. The two most common infections exerting notable airway narrowing are tuberculosis and fibrosing mediastinitis. Initial diagnostic work-up begins with a chest radiography, but the gold-standard investigative technique is CT scan. Large airways' involvement by TB occurs either by direct extension of the infection to the tracheal wall through the lymphatic system or from external compression by enlarged lymph nodes. Usual locations are the distal trachea and proximal main bronchi (Figs 13 and 14). Direct large airway involvement by TB typically appears as edematous wall thickening along with tuberculous granulations projecting intramurally. Fibrosing mediastinitis is characterized by abnormal fibrous tissue proliferation in the mediastinum. Histoplasma capsulatum infection is the most common cause of fibrosing mediastinitis in children. On CT, it presents as focal or diffuse disease. The focal pattern appears as a soft tissue mass with calcifications, most commonly in the right paratracheal, subcarinal, or hilar regions. The diffuse form is characterized by a diffusely infiltrating mass without the presence of calcifications affecting entire mediastinal compartments, and can be associated with other fibrosing disorders such as retroperitoneal fibrosis. Inflammatory pseudotumor of the

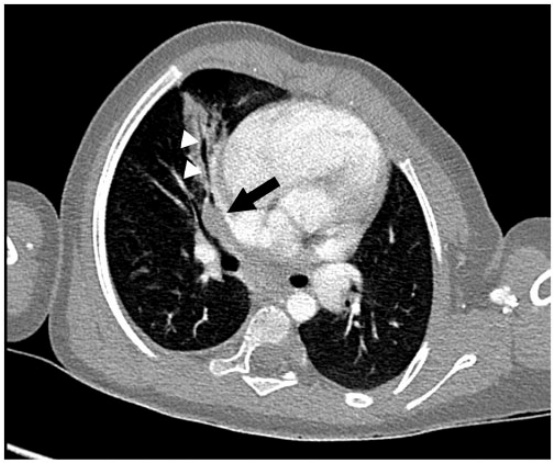

Fig. 14. Mediastinal lymphadenopathy on a 3-year-old girl due to *Mycobacterium avium* complex (MAC) infection. Oblique axial CT image shows a tumorous lesion (black arrow) obstructing the beginning of the medial segmental bronchus, along with the consolidation of the peripheral lung parenchyma and air bronchogram sign (arrowheads), which ultimately histologically proved to be, after middle lobe excision, lymphadenopathy from MAC infection. $CTDI_{vol} = 2.7$ mGy.

lung constitutes a lesion of unknown etiology, with no malignant potential which mimics a tumorous mass. Its symptomatology is inconspicuous, including fever, cough, shortness of breath, chest pain, and sputum. Initial investigation starts with a chest radiography, followed by a CT scan, on which it appears as a solitary, well-demarcated round or oval nodule or mass. Calcifications, cavitation, and heterogeneous attenuation with non-specific pattern of contrast enhancement can also be noted.[1,3,5,6,24–26]

Conclusion

Modern imaging modalities enable fast, easy, and accurate assessment of large airway pathology especially in pediatric patients, thus making large airway diseases part of the daily routine for pediatric radiologists, with which they should be familiar.

Declaration of Conflicting Interests

The author(s) declared no potential conflicts of interest with respect to the research, authorship, and/or publication of this article.

Funding

The author(s) received no financial support for the research, authorship, and/or publication of this article.

ORCID iD

Spyridon Prountzos https://orcid.org/0000-0001-9651-8338

References

1. Chassagnon G, Morel B, Carpentier E, et al. Tracheobronchial branching abnormalities: lobe-based classification scheme. Radiographics 2016;36:358–373.
2. Papaioannou G, Young C, Owens CM. Multidetector row CT for imaging the paediatric tracheobronchial tree. Pediatr Radiol 2007;37:515–529.
3. Lee EY, Greenberg BS, Boiselle PM. Multidetector computed tomography of pediatric large airway diseases: state-of-the-art. Radiol Clin N Am 2011;49:869–893.
4. Ghaye B, Szapiro D, Fanchamps JM, et al. Congenital bronchial abnormalities revisited. Radiographics 2001;21:105–119.
5. Semple TT, Calder A, Owens CM, et al. Current and future approaches to large airways imaging in adults and children. Clin Radiol 2017;27:356–374.
6. Heidinger BH, Occhipinti M, Eisenberg RL, et al. Imaging of large airways disorders. AJR 2015;205:41–56.
7. Javia L, Matthew HA, Fuller A. Rings, slings, and other tracheal disorders in the neonate. Semin Fetal Neonatal Med 2016;21(4):277–284.
8. Lee EY, Zucker EJ, Restrepo R, et al. Advanced large airway CT imaging in children: evolution from axial to 4-D assessment. Pediatr Radiol 2013;43:285–297.
9. Alamo L, Vial Y, Gengler C, et al. Imaging findings of bronchial atresia in fetuses, neonates and infants. Pediatr Radiol 2016;46:383–390.
10. Stagnaro N, Rizzo F, Torre M, et al. Multimodality imaging of pediatric airways disease: indication and technique. Radiol Med 2017;122: 419–429.
11. Smith BM, Lu JC, Dorfman AL, et al. Rings and slings revisited. Magn Reson Imaging Clin N Am 2015; 23:127–135.
12. Browne LP. What is the optimal imaging for vascular rings and slings? Pediatr Radiol 2009;39:191–195.
13. Acharya PT, Ali S, Stanescu AL, et al. Pediatric mediastinal masses: role of MR imaging as a problem-solving tool. Magn Reson Imaging Clin N Am 2019;27:227–242.
14. Garcıa-Guereta L, Garcıa-Cerro E, Bret-Zurita M. Multidetector computed tomography for congenital anomalies of the aortic arch: vascular rings. Rev Esp Cardiol 2016; 69:681–693.
15. Achint K, Sargar K, Restrepo CS. Pediatric mediastinal tumors and tumor-like lesions. Semin Ultrasound CT MRI 2016;37:223–237.
16. Wallis C, Alexopoulou E, Antón-Pacheco JL. ERS statement on tracheomalacia and bronchomalacia in children. Eur Respir J 2019;54:1900382.
17. Goo HW. Four-dimensional thoracic CT in free-breathing children. Korean J Radiol 2019;20(1):50–57.
18. Douros K, Kremmydas G, Grammeniatis V, et al. Helical multi-detector CT scan as a tool for diagnosing tracheomalacia in children. Pediatr Pulmonol 2019;54:47–52.
19. Cutrone C, Pedruzzi B, Tava G, et al. The complimentary role of diagnostic and therapeutic endoscopy in foreign body aspiration in children. Int J Pediatr Otorhinolaryngol 2011;75:1481–1485.
20. Gibbons AT, Casar Berazaluce AM, Hanke RE, et al. Avoiding unnecessary bronchoscopy in children with

suspected foreign body aspiration using computed tomography. J Pediatr Surg 2020;55:176–181.
21. Rybojad B, Niedzielska G, Rudnicka-Drożak E. Diagnosis of paediatric airway foreign body: is it easy? Cent Eur J Med 2014;9:648–652.
22. Kashif R, Faizan M, Anwar S. Pediatric malignant mediastinal masses. J Coll Physicians Surg Pak 2019;29:258–262.
23. Manson DE. Magnetic resonance imaging of the mediastinum, chest wall and pleura in children. Pediatr Radiol 2016;46:902–915.
24. Chiappini E, Lo Vecchio A, Garazzino S, et al. Recommendations for the diagnosis of pediatric tuberculosis. Eur J Clin Microbiol Infect Dis 2016;35:1–18.
25. Garcia-Peña P, Guillerman PR. Pediatric chest imaging. Berlin Heidelberg: Springer-Verlag, 2014.
26. Arkoudis N-A, Pastroma A, Velonakis G, et al. Solitary round pulmonary lesions in the pediatric population: a pictorial review. Acta Radiol Open 2019;85:1–12.